Journal of Fluorescence, Vol. 4, No. 4, 1994

Analysis of Cell Surface Molecular Distributions and Cellular Signaling by Flow Cytometry

J. Matkó,[1] L. Mátyus,[1] J. Szöllősi,[1] L. Bene,[1] A. Jenei,[1] P. Nagy,[1] A. Bodnár,[1] and S. Damjanovich[1,2]

Received October 18, 1993

Flow cytometry is a fast analysis and separation method for large cell populations, based on collection and processing of optical signals gained on a cell-by-cell basis. These optical signals are scattered light and fluorescence. Owing to its unique potential of *statistical data analysis and sensitive monitoring of (micro)heterogeneities in large cell populations,* flow cytometry—in combination with microscopic imaging techniques—is a powerful tool to study molecular details of cellular signal transduction processes as well. The method also has a widespread clinical application, mostly in analysis of lymphocyte subpopulations for diagnostic (or research) purposes in diseases related to the immune system. A special application of flow cytometry is the mapping of molecular interactions (proximity relationships between membrane proteins) at the cell surface, on a cell-by-cell basis. We developed two approaches to study such questions; both are based on *distance-dependent quenching of excited state fluorophores (donors) by fluorescent or dark (nitroxide radical) acceptors* via Förster-type dipole-dipole resonance energy transfer (FRET) and long-range electron transfer (LRET) mechanisms, respectively. A critical evaluation of these methods using donor- or acceptor-conjugated monoclonal antibodies (or their Fab fragments) to select the appropriate cell surface receptor or antigen will be presented in comparison with other approaches for similar purposes. The applicability of FRET and LRET for two-dimensional antigen mapping as well as for detection of conformational changes in extracellular domains of membrane-bound proteins is discussed and illustrated by examples of several lymphoma cell lines. Another special application area of flow cytometry is the analysis of different aspects of cellular signal transduction, e.g., changes of intracellular ion (Ca^{2+}, H^+, Na^+) concentrations, regulation of ion channel activities, or more complex physiological responses of cell to external stimuli via correlated fluorescence and scatter signal analysis, on a cell-by-cell basis. This way different signaling events such as changes in membrane permeability, membrane potential, cell size and shape, ion distribution, cell density, chromatin structure, etc., can be easily and quickly monitored over large cell populations with the advantage of revealing microheterogeneities in the cellular responses. Flow cytometry also offers the possibility to follow the kinetics of slow (minute- and hour-scale) biological processes in cell populations. These applications are illustrated by the example of complex flow cytometric analysis of signaling in extracellular ATP-triggered apoptosis (programmed cell death) of murine thymic lymphocytes.

KEY WORDS: Fluorescence; flow cytometry; electron transfer; energy transfer; cell surface; protein association; signal transduction.

FLOW CYTOMETRY: BASIC PRINCIPLES, INSTRUMENTATION

Quantitative analysis of physical parameters of cell populations has always been important in research. Flow cytometry is one possible approach that, besides being extensively utilized in research, has become a common tool in clinical laboratories as well [1–14]. In this paper we briefly discuss the underlying principles and review the most important applications, with special respect to characterizing inter- and intramolecular distances of cell surface proteins. Several aspects of transmembrane signaling is also discussed.

[1] Department of Biophysics, University School of Medicine, 4012 Debrecen, Hungary.

[2] To whom correspondence should be addressed.

1053-0509/94/1200-0303$07.00/0

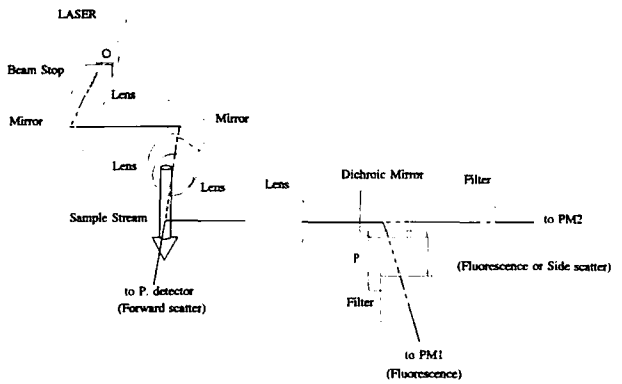

Fig. 1. Generalized scheme of a flow cytometer.

The basic structure of flow cytometers is similar, although there are great variations in the actual design (Fig. 1 shows a generalized block diagram of a flow cytometer). The sample, a suspension of single cells, is delivered to a nozzle or flow chamber through tubings under pressure. In a typical system the sample suspension is led through the center of the orifice of the nozzle or through the center of the flow chamber. Direct contact of the cells with the orifice would destroy them, therefore hydrodynamic focusing is used to keep the cells centered in the fluid stream. Hydrodynamic focusing is achieved by another fluid system, the so-called sheath fluid, which surrounds the sample stream. The dimensions of the flow systems and the pressure in them – consequently the velocities of both fluid streams – are carefully designed, therefore no turbulence occurs in either of them. The cells travel through the flow chamber or leave the orifice of the nozzle in single file. A few millimeters away from the nozzle or within the flow chamber the cell is illuminated with focused monochromatic light coming from a laser or from a noncoherent light source. In more sophisticated instruments two or even three lasers are used for excitation, allowing multiparameter analysis. Optical signals are detected from each cell by appropriate detector systems: photodiodes or photomultiplier tubes. Light-scatter, absorption, and fluorescence are the commonly measured optical parameters. The light-scatter detector can be placed either parallel or perpendicular to the excitation beam. In the former case we speak about forward-angle light scatter (FALS), while the latter is called 90° light scatter or side-scatter. The absorption detector is placed in the path of the excitation beam, while the fluorescence detector is orthogonal or, in very special situations, parallel to the excitation beam. Optical filters are placed in front of the fluorescence detectors in order to separate two fluorescence signals emitted by the different dyes. The analog signals coming from the detectors are first amplified and then digitized using analog–digital converters. Both the height of the pulses (peak signal) and the area under them (integrated signal) can be used for the conversion. Some older instruments detect signals that are a mixture of the peak and integrated signals owing to the slower response time of the electronics. The digital data are usually stored in so-called list mode files. The list mode file contains the values of each measured parameter grouped together according to individual cells. The data can be processed further; one- and two-parameter plots can be generated. A one-parameter plot is a relative frequency distribution, where the X axis is proportional to the intensity of the signal and the Y axis indicates the number of cells having a given signal. In a two-parameter plot the cells are represented as dots positioned according to the value of the parameter belonging to the respective axes. Two-parameter plots can also be visualized as contour plots or three-dimensional plots, where the height is proportional to the cell number. Gating is an often-used procedure in data evaluation, where data analysis is restricted to cells with parameter values falling in specified ranges according to one or more parameters. Gating can also be done electronically during the data collection, but gating on list mode files is preferred, because it allows data analysis according to different combinations of gates.

Since the duration of illumination typically is a few microseconds and the signal processing is even shorter, considerably high rates of data acquisition can be achieved. It is therefore possible to collect data on several different parameters of each of 100,000 cells in a few minutes. Indeed, the currently applied data processing and collecting systems do not limit the speed of the measurements [15].

PARAMETERS OF FLOW CYTOMETRY

Light Scatter

Although the light scatter signal is measured in every flow cytometer, it is mainly used only as a trigger signal to initiate the collection of fluorescence, because the light scatter signals are relatively unspecific for cellular properties. Discrimination among many cell types is possible, based on the side-scatter and FALS intensities. Debris and unwanted cells can be eliminated from the data collection by gating on the scatter signals. The FALS signal is related to cell size, assuming spherical cells, though the internal refractive index of the cells affects their scatter signal. Asymmetric cells give a het-

erogeneous FALS signal, because the cells pass the detector at different orientations. The FALS signal is relatively insensitive to the internal structure of cells, but the side-scatter increases with the cells' granularity.

Fluorescence

Fluorescence intensity measurements are based on the "central dogma of flow cytometry," i.e., the signal intensity is proportional to the concentration or amount of fluorophore of interest. It generally applies, but the possibility of artifacts should always be considered. Since so many applications of fluorescence measurements are possible in flow cytometry and excellent reviews are available, we do not try to cover all of them [1–15]. We limit our discussion to methods for studying cell surface proteins and some aspects of signal transduction.

IMMUNOFLUORESCENCE MEASUREMENTS

Cells express many antigens on the surface of the cytoplasmic membrane characterizing the cell type or the functional state of the cell. The presence and also the density of a specific cell surface molecule can be determined by flow cytometry. Cell surface antigens can be identified by specific antibodies. A broad selection of polyclonal and monoclonal antibodies is available from several companies. Fluorophores can be conjugated directly to the antibody (direct immunofluorescence) or to a second antibody directed against the first antibody (indirect immunofluorescence). Instead of the second antibody, streptavidin, a 60-kD protein of *Streptomyces avidinii* having four biotin binding sites, also can be used. In this case the first antibody should be coupled to biotin. Useful fluorophores can be excited at the wavelength of the available light source and have a high quantum efficiency and a large Stokes shift. Naturally, the dye should contain a functional group, through which it can be coupled to immunoglobulins or to streptavidin.

Fluorescein isothiocyanate (FITC) is the most commonly used fluorophore for immunofluorescence. It can be excited by the 488 nm line of an argon ion laser as well as with a mercury arc lamp (at 415 nm). It can easily be conjugated to antibodies without diminishing their binding activity. FITC-conjugated antibodies can be applied together with propidium iodide (an intercalating DNA stain) staining. Both can be excited by the 488 nm line of argon ion lasers. The relatively small spectral overlap allows the independent detection of these dyes.

Tetramethylrhodamine isothiocyanate (TRITC) is well excitable with mercury arc lamps (565 nm line). Although the 514 nm line of argon ion laser is suboptimal, it gives satisfactory results. For multiparameter flow cytometry, when several surface antigens are labeled simultaneously, other dyes are necessary. Other rhodamine derivatives, such as Texas Red and X-RITC are suitable, because both their excitation and their emission spectra are shifted toward longer wavelengths. X-RITC decreases somewhat the water solubility of the IgG; Texas Red is better from this point of view. Cy3 is a member of the new generation of fluorescent dyes, having advantages over the above-mentioned dyes. It is more hydrophilic and does not cause nonspecific binding or aggregation. It can be advantageously applied in combination with fluorescein-conjugated antibodies in double-labeling experiments, however, narrow-band optical filters should be used for better discrimination.

A new family of red-emitting dyes was introduced a few years ago. Phycobiliproteins are prepared from cyanobacteria and red algae. The most useful members of this family are B-phycoerythrin, R-phycoerythrin, C-phycocyanin, and allophycocyanin. Although their molecular weight is 100–200 kD, they can be applied well, because their molar extinction coefficients are over a million, with quantum yields nearly 1. Several other properties make them valuable for immunofluorescence studies: their broad excitation spectra, large Stokes shift, and water solubility and the fact that their fluorescence intensity is relatively insensitive to pH. Thus they are suitable for visualizing antigens expressed at an extremely low density. Phycobiliproteins, owing to their size, are less useful than fluorescein or rhodamines in fluorescence energy transfer measurements.

To increase the available selection of fluorochromes, a whole series of so-called tandem dyes are synthesized. Tandem fluorochromes consist of two dyes, of which the first serves as a donor transferring the excitation energy to the other (acceptor) dye by nonradiative mechanism. The first tandem conjugate, consisting of R-phycoerythrin and allophycocyanin, was described by Glazer and Stryer [16]. Recently several other organic dyes have been applied as acceptor, such as Texas Red and Cy5. The latter is called Quantum Red.

In multiparameter studies a recently introduced dye, the peridinin chlorophyll protein, (PerCP), might gain widespread application [17]. It is a red fluorescent pigment of the photosynthetic accessory system of dinoflagellates with a wide absorption band (400–550 nm) and a large Stokes shift (200 nm).

Autofluorescence, a general property of cells, causes a background fluorescence signal. It becomes disturbing when specific low-intensity signals are to be detected, thus limiting the resolution of the system. Cellular autofluorescence has broad excitation and emission spectra. It is caused mainly by nicotinamide adenine dinucleotide (NADH), riboflavin, and flavin coenzymes [18,19]. Unfortunately it cannot be eliminated by any nontoxic procedure, though its intensity varies with different cell growth conditions. Different methods have been elaborated for making a correction for autofluorescence. The simplest is to subtract the average background fluorescence intensity from each measured signal, however, the large deviations from the mean result in errors in the correction. Methods based on dual-laser excitation or the detection of fluorescence at multiple spectral regions offer the possibility to make the correction on a cell-by-cell basis [20–23].

A similar experimental error is caused by the spectral overlaps of the emission ranges of simultaneously applied dyes. Most commercial instruments have built-in fluorescence compensation electronics. Since the signal is a function of the photomultiplier voltage and the amplification, the correction factors have to be determined for each experiment. Fluorescence compensation can also be done by computers using list mode files.

ANALYSIS OF PROTEIN DISTRIBUTIONS AT THE CELL SURFACE BY MEANS OF FLOW CYTOMETRIC LUMINESCENCE QUENCHING TECHNIQUES

Studies of Intercellular Communication

Intercellular communication has many features among identical or different types of cells, but undoubtedly it is a key element of interactions between immunocompetent cells. The communication itself depends on specific recognition processes among particular cell surface molecules. Of course, the localization and proximity (aggregational) relationship of these specific interacting molecules in the plasma membrane is of great interest. Fluorescence resonance energy transfer has the capacity to reveal proximity relationships between cell surface molecules, properly labeled with fluorescent donor–acceptor pairs.

The specific targeting by the fluorescent labels can be carried out in particularly favorable cases directly on the target molecules. In the general case, however, different forms of monoclonal antibodies serve the targeting.

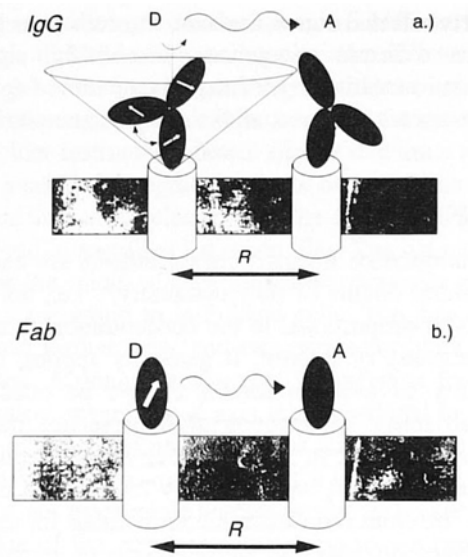

Fig. 2. Labeling of cell surface proteins by antibodies. (a) Whole antibody (IgG): More than one dye per antibody + randomization of dipoles by segmental (hinge-bending) motions. (b) Fab fragments: About one dye per Fab + a relatively rigid and compact tertiary structure.

Methods to Study Cell Surface Patterns

Chemical cross-linking, immunoprecipitation, electron microscopy, and, e.g., atomic force microscopy, have the "resolution power" to distinguish between macromolecules and receptor molecules in each others' vicinity or unrelated entities. Fluorescence energy transfer offers a great advantage, namely, it can determine distance relationships between molecular elements of the cell surface of living cells and, in a fluorescence cell analyzer-sorter, all these over a large cell population or selected subpopulations, on a cell-by-cell basis, in a short time interval. The method itself has been reviewed extensively, but little analysis has been performed on the differences of Fab or whole-antibody labeling. Figure 2 depicts the basic differences between size and mobility of Fab and IgG molecules.

Before analyzing the potential advantages of applying Fab fragments or whole antibodies, we have to outline at least the very basic features of distance-dependent luminescence quenching measurements. Here we restrict ourself to two approaches, Förster-type resonance energy transfer [24] and long-range electron transfer [25].

Förster-Type Resonance Energy Transfer: Data Evaluation and Interpretation

The transfer efficiency (E) for a Förster-type singlet–singlet resonance excitation energy transfer between

a properly selected donor–acceptor pair can be expressed as

$$E = \frac{k_t}{k_t + k_f + \Sigma k_i} \quad (1)$$

where k_t and k_f are the rate constants for energy transfer and donor fluorescence, respectively, while Σk_i is the sum of rate constants of all other nonradiative deexcitation processes in the excited donor molecules. The fluorescence quantum efficiency in the presence of an acceptor is given by

$$\frac{\varphi_{D+A}}{\varphi_D} = 1 - E \quad (2)$$

The dependence of k_t on the relative orientation and the distance between the emission dipole of the donor and the absorption dipole of the acceptor can be expressed as

$$k_t = dJk_f n^{-4} R^{-6} \kappa^2 \quad (3)$$

where d is a composite constant whose value depends on the choice of units and J is the spectral-overlap integral between the normalized emission spectrum of the donor molecule and the absorption spectrum of the acceptor weighted by the fourth power of the wavelength:

$$J = \frac{\int F_D(\lambda)\, \varepsilon_A(\lambda)\, \lambda^4 d\lambda}{\int F_D(\lambda)\, d\lambda} \quad (4)$$

where F_D is the emission intensity per unit wavelength interval of the donor fluorescence at the wavelength λ and $\varepsilon(\lambda)$ is the molar absorbance of the acceptor at the same wavelength. In Eq. (3), n is the refractive index of the medium between donor and acceptor chromophores, R is their separation, and κ^2 is a measure of the relative orientation among the emission dipole of the donor, the absorption dipole of the acceptor, and their separation vector, defined by

$$\kappa^2 = (\cos\Theta - 3\cos\omega_1 \cos\omega_2)^2 \quad (5)$$

The angles of θ, ω_1, and ω_2 describe the relative orientation of the donor–acceptor pair in three dimensions. Equation (3) can be rewritten as

$$k_t = C\kappa^2 R^{-6} \quad (6)$$

where C contains all constant parameters for the given donor–acceptor pair.

As has become well established, resonance energy transfer technique is a practical method for establishing separations between donor and acceptor molecules at the level of several to several tens of nanometers [26,27]. This has been widely exploited in "spectroscopic ruling" [28] as a method of obtaining conformational information on isolated macromolecules and their complexes labeled at specific sites or randomly over their surfaces [29]. At the other extreme it can also provide topological information on acceptor-labeled species in random two- or three-dimensional arrays via its capacity to estimate their local concentrations [30]. These, coupled with independent estimates of overall concentrations, may indicate the presence of nonrandom localization, exemplified, for example, by domain formation and specific interactions [31] or ligand-induced aggregation [32].

In the case of mapping out the topology of cell surface antigens by energy transfer using fluorescently labeled monoclonal antibodies, each mAb is randomly labeled by a small number of fluorescent dyes. These are bound mostly to the ε-amino groups of the lysyl moieties. This structural arrangement of the fluorescent dyes may not be enough definitively to establish more than changes in separations and/or relative orientations, or their distributions, as opposed to realistic absolute estimates of these parameters [33]. Additionally, the measurements will yield transfer efficiencies averaged over individual cells, if carried out under a microscope or by flow cytometry. They will be averaged still further over a somewhat heterogeneous cell population if the measurements are carried out in cuvettes, in which case they may also be distorted by the presence of cell debris.

The importance of the kappa square factor in determining the actual distances between particular membrane elements is obvious.

Long-Range Electron Transfer: Another Intra- and Intermolecular Ruler Applicable to Cell Surfaces by Means of Flow Cytometry

This approach is based essentially on an electron transfer reaction between an electron donor and an electron acceptor molecule being within a "sphere of action". The rate and distance interval of quenching are highly dependent on the redox potential of the donor and acceptor molecules and on the nature of the intervening medium as expressed by the famous Marcus theory of electron transfer [25,34]:

$$k_{ET} = A\exp\left(-\frac{\Delta G^*}{RT}\right) \quad (7)$$

where k_{ET} is the rate of the electron transfer, A is a preexponential factor, ΔG^* is the free energy of activation,

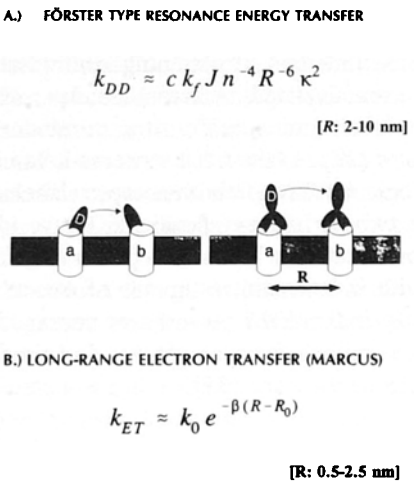

Fig. 3. Distance-dependent luminescence quenching methods for cell surface mapping.

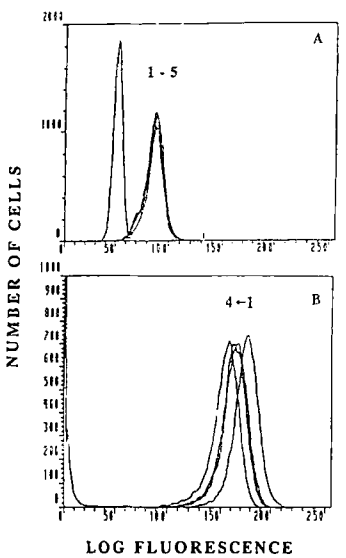

Fig. 4. Flow cytometric long-range electron transfer quenching (LRETQ) measurements at the surface of human lymphocytes. (A) Resting peripheral blood B lymphocytes: The cytogram on the left shows the autofluorescence of cells, while cytograms 1–5, on the right, show the fluorescence of FITC-anti HLA I-labeled cells at gradually increasing nitroxide (quencher)-anti HLA I fractional cell surface densities. (B) Virus-transformed B lymphoblasts (JY): The cytogram on the left shows the autofluorescence, while cytograms 1–4, on the right, were recorded on JY cells labeled with FITC-anti HLA I at gradually increasing fractional cell surface densities of nitroxide-HLA I (from right to left).

which is related to the free energy of the redox reaction, ΔG^o, and the reorganization energy (internal + solvent shell), λ, as follows:

$$\Delta G^* = \lambda/4\,(1 + \Delta G^o)^2 \qquad (8)$$

Besides recognizing this unusual quadratic dependence of the activation free energy on the free energy of the redox reaction, Marcus [34] and Dexter [35] predicted an exponential dependence of the electron transfer rate on the donor–acceptor separation distance:

$$k_{ET}\,(R) = k_o \exp\,[-\beta\,(R-R_o)] \qquad (9)$$

where k_o is the rate at the van der Waals contact distance, R_o, while β is the factor characterizing the steepness of the distance dependence, and R is the actual separation distance between the donor and the acceptor. The effective range of ET distances is often strongly influenced (extended) by opening of effective electron-tunneling pathways, e.g., through polypeptide backbones or polyhydroxy (carbohydrate) moieties of cell surface macromolecules [36].

The predictions by Marcus and Dexter have been nicely verified by experimental observations on different natural [37,38] and semisynthetic systems [39–41]. This provides a potential application for long-range electron transfer (LRET) as an inter- or intramolecular ruler in the distance range of 0.5–2.5 nm (Fig. 3). Application of LRETQ to cellular systems has two obvious advantages. The quenching experiments require measurements only on the donor side, therefore the method can be regarded as a very fast screening of physical association of membrane proteins. On the other hand, the narrow range of effective ET distances as well as the reduced sensitivity to the spatial orientation of the donor and acceptor molecules makes the approach extremely powerful in detecting protein clustering at the cell surface by means of flow cytometry or microscopic imaging techniques.

The methodical background of LRETQ measurements on living cells has been described very recently, in detail [42]. This approach has been successfully applied to monitor homoassociations of class I MHC molecules on a large number of human lymphoid cells [43,44] in good accordance with FCET or immunoprecipitation data obtained under the same conditions.

Here we illustrate the application of flow cytometric LRETQ with the example of MHC self-association on resting human peripheral B lymphocytes (Fig. 4A) and transformed human B lymphoblasts (Fig. 4B). The flow cytograms, recorded in the absence and at increasing surface densities of nitroxide-conjugated antibodies, nicely demonstrate a lack of self-association of cell surface MHC I molecules on resting HP B lymphocytes at a low expression level, while the MHC I shows a high degree of self-association on the B lymphoblasts at a higher level of surface expression.

The Question of the Tag: How to Visualize Membrane Proteins?

Except in several lucky situations, such as the Band 3 protein in the human erythrocyte membrane [45] or the Ca^{2+}-ATPase enzyme in the SR or cytoplasmic membranes [46], the majority of the membrane proteins cannot be directly labeled by selective chemical modification. This means that, in most cases, "tagging" of membrane proteins requires development of specific monoclonal antibodies against the membrane protein under study. Then one can use fluorophore- or dark acceptor (quencher)-conjugated whole immunoglobulin molecules (most frequently IgG isotypes) or Fab fragments prepared by papain digestion of IgG [47].

Now let us analyze the question whether the whole antibody and the Fab fragment behave similarly or whether either of them offers an advantage over the other.

(i) Whole IgG molecules, depending on their idiotypes, have nearly a hundred ε-amino groups (lysyl sidechains) as potential donor- or acceptor-dye binding sites, to which the fluorophore molecules are generally covalently linked through isothiocyanate moieties. Fab fragments contain less than one-third lysyl side chains. This fact puts the IgG in favor over Fab, because of the higher signal level and expectedly better fulfillment of the dynamic averaging condition. The latter is due to a much higher probability of having *more, and more mobile, binding sites for the labels in the case of whole antibodies than for Fab fragments.*

(ii) Fab fragments are significantly smaller molecules with minimal internal flexibility, which means a *higher accuracy in functioning as a ruler.*

(iii) An important question is the *perturbation of the cell surface architecture (and cellular function) by the antibody binding* itself. Fab fragments are not supposed to trigger any cellular processes which may lead to molecular aggregation in the plasma membrane, thereby generating evoked proximity relationships. In contrast, bivalent IgG molecules, in some cases, may dimerize nearby molecules in the plasma membrane, through binding their epitopes with the identical hypervariable sites of the antibody. In such cases it can immobilize very likely only preexisting homodimers (or their complexes with other proteins), since it is unlikely that heterogenic antigens carry the same epitopes. This would question the basic principle of the monoclonality. Such heterodimers certainly will not enhance the measured energy transfer efficiently, since it depends only on the acceptor concentration. It is obvious that the determined donor–acceptor distance will be the same as for monomeric donors.

(iv) In conclusion, the application of singlet–singlet resonance energy transfer measurements to determine proximity relationships can be done with whole antibodies or Fab fragments. However, the type of antibody, labeled cell surface antigen, and spectroscopic requirements have to be considered for each particular case. These together will influence the decision of whether whole antibody or Fab fragments are the preferred tags for the spectroscopic measurements.

Cell Surface Protein Patterns

Flow cytometric energy transfer measurements helped to describe nonrandom codistribution patterns of protein molecules, where this codistribution is not justified by their overall density in the plasma membrane, assuming a Poisson-type distribution of the molecules and a sphere-like cell model.

The method itself was first applied by Chan *et al.* [48] and further developed by us in collaboration with Drs. Jovin and Arndt-Jovin [31,49,50]. Table I shows the list of proximities determined so far between different cell surface antigens. Under normalized conditions (for dye-to-antibody and antigen-to-antigen ratios), the relative proximities may allow us to construct two-dimensional models of non-randomly codistributed antigen groups. Of course, in this case the third dimension, i.e., the length of the molecule in the extracellular space must be neglected. Nevertheless, since antibodies generally have a comparable or even a larger size than membrane-bound cell surface molecules, this can be accepted as a first approximation, yet to be confirmed by other more direct methods. These could be, in principle, atomic force microscopy or, e.g., tunneling electron microscopy. These methodical approaches have, however, the unavoidable handicap that they cannot provide the distribution of such parameters over a cell population.

In light of the above discussion, we can conclude that flow cytometric resonance energy transfer (FCET) or LRETQ measurements both have the capacity to detect homo- or heteroassociations of donor–acceptor pair labeled cell surface proteins.

Detection of Conformational Changes in the Extracellular Domains of Membrane Proteins by Means of Flow Cytometry

The two distance-dependent quenching techniques discussed above are both able to detect conformational changes in the extracellular domains of large integral membrane proteins through intramolecular quenching processes. In the case of intramolecular quenching the

Table I. Selected Applications of Flow Cytometric Energy Transfer to Cell Surface Mapping[a]

Donor (determinant)	Acceptor (determinant)	Result proximity (<*E*>, %)	Cell	Ref. No.
F—ConA	R—ConA	++	Friend erythroleukemia	48
		++	HL—60 leukemia	70
		+	HK—22 murine lymphoma	31,49,71
		+	Normal mouse lymphocytes	71
		+	Gross virus leukemic mouse lymphocytes	71
F—anti-H-2K^k	R—anti-H-2K^k	−	LDBH T41 mouse lymphoma	72
F—anti-Tac (IL-2R)	R—OKT27 (ICAM-I)	+ (7.3)	HuT 102B2 T lymphoma	73
F—anti-Tac	R—anti-TfR	−		
F—OKT27	R—OKT27	+ (10.0)		
F—anti-TfR	R—anti-TfR	+ (8.4)		
F—OKT27	R—anti-TfR	−		
F—anti-TfR	R—OKT27	−		
F—L368 (β_2-microglobulin)	R—L368	−		
F—anti-Tac	R—W6/32 (HLA-A,B,C)	++ (11.0)		
F—OKT27	R—W6/32	+ (7.0)		
F—L243 (HLA-DR)	R—W6/32	++ (11.2)	PGF B lymphoblast (JY lymphoblast)	74
F—Leu10 (HLA-DQw1,3)	R—W6/32	++ (12.2)		
F—Leu10	R—Leu10	++ (10.4)		
F—anti-HLA-I	R—anti-CD4	−	Human T lymphocytes	75
F—anti-p55-IL2-R	R—anti-HLA-I	+		
F—anti-InsR	R—anti-H2(K,D,L)	++ (~20)	NIH 3T3 HIR 3.5	76
F—anti-CD4	R—anti-CD3	+ (9.4)/37°C/; −/4°C/	Murine T cell hybridomas	77
F—anti-CD45	R—anti-CD3	−		
F—OKT4D (CD4)	R—anti-CD45	++ (time dependent)	Anti-CD3-Ti-activated or MLR-activated PB T lymphocytes	78
F—OKT8 (CD8)		+ (time dependent)		
F—W6/32 (HLA-I)		−		
F—anti-CD45		−		
F—HLA-A2	Texas Red—HLA-A2	++ (17.0) (β_2 dependent)	DMPC, SL liposomes	44
F—anti-aminopeptidase N	R—anti-aminopeptidase N	+	Brush border and basolateral membrane vesicles	79

[a]F, FITC; R, TRITC. (+) 5% ≤ <*E*> ≤ 10%; (++) <*E*> > 10%; (−) <*E*> < 5%.

two membrane proteins are labeled at two distinct epitopes by fluorophore- or quencher-conjugated antibodies (or with their Fab fragments).

If the distance between the labels attached to the two binding sites are within the effective distance range of Förster-type resonance energy transfer or Marcus-type electron transfer, then small displacements of protein residues, segments, or even domains can be monitored due to the steep distance dependence of both quenching rate [39,40,42]. In such types of experiments the flow cytometry offers the advantage of statistical interpretation and the chance to explore microheterogeneities in the conformational responses in large cell populations.

SELECTED APPLICATIONS OF FLOW CYTOMETRY IN ANALYSIS OF CELLULAR SIGNAL TRANSDUCTION

Signal transduction is a series of physical and chemical events occurring when information arriving from extracellular space is transferred through the cytoplasmic membrane inside the particular cell [51]. There are numerous membrane-linked physicochemical changes in the cells induced by triggering molecules bound to specific membrane receptors or perturbing the membrane directly, such as changes in membrane permeability, lipid fluidity, membrane potential, transient or sustained elevations of intracellular ion concentrations

Table II. Selected Applications of Flow Cytometry to Analysis of Cellular Signal Transduction[a]

Cellular parameter	Probe	Excitation/emission maximum (nm)	Molecular basis of the optical signal	Biological problem(s)
Membrane potential	Carbocyanine dyes [diOC$_n$(3)]	484/510	Potential-dependent dye redistribution	Cell activation, programmed cell death (PCD)
	Oxonol dyes [diBaC$_4$(n)]	490/520		
	Rhodamine-123	505/534		
Cell surface protein expression	FITC-NH-Ab	490/520	Density-dependent emission intensity	Cell activation, immunodiagnostics, immunmodulation
	TRITC-NH-Ab	554/573		
	Texas Red-NH-Ab	596/620		
	Phycoerythrin-R	480–565/578		
	Allophycocyanine	650/660		
pH	6-Carboxyfluorescein	495/520	Spectral shift	Cell activation, PCD
	BCECF	505/530		
	SNAFL	547/630		
Intracellular calcium	Fura-2 (ratio mode)	335/512–518	Spectral shift and/or change in quantum yield	Cell activation, PCD
		360/505–510		
	Indo-1 (ratio mode)	330/390–410		
		350/482–485		
	Fluo-3	464/526		
Intracellular sodium	SBFI	396/570	Spectral shift and/or change in quantum yield	Cell activation, PCD
Membrane permeability	FDA	490/520	Binding to nucleic acids after passing the cytoplasmic barrier	PCD
	Propidium iodide	536/623		
	Etidium bromide	510/595		
	Acridine orange	480/520		
		440–470/650		
Cell volume	—	—	Forward-angle light scattering	Apoptosis, cell activation
Cell density/granularity	—	—	90° light scattering	Apoptosis, cell activation

[a]Sources: Refs. 52–57 and 64–67.

(Ca^{2+}, Na^+), or cytosolic acidification or alkalinization (ΔpH). Besides this, the cells may undergo several striking morphological changes such as changes in their volume or density (granularity) or changes in the chromatin structure. Flow cytometry offers a simple and ultrafast method to analyze these cellular responses upon cell activation or triggering of cell death over large cell populations with the possibility of heterogeneity analysis. *Table II* lists several major application areas of flow cytometry in the analysis of transmembrane signaling. We note that excellent, detailed reviews are available on the technical questions [52,53] and also on the fluorescent probes available for flow cytometric signal transduction analysis [54–57]. Thus, in the next paragraphs we try to focus on a brief demonstration of several unique features of flow cytometry in exploring the biphasic (or multiphasic) character of cellular responses or in following the kinetics of complex signaling processes such as programmed cell death (apoptosis).

Membrane Potential and Permeability

Flow cytometric membrane potential measurements are based on detection of changes in cell fluorescence induced by potential-dependent redistribution of dyes between membrane and aqueous phases [58]. The application of *carbocyanine and oxonol* dyes to flow cytometry allows sensitive monitoring of hyper- or depolarization of the plasma membrane in various cells and detection of heterogeneities within cell populations [50,58]. Figure 5 demonstrates the biphasic nature of membrane-potential changes induced by extracellular ATP on murine thymic lymphocytes depending on the concentration and incubation time, as revealed by ox-

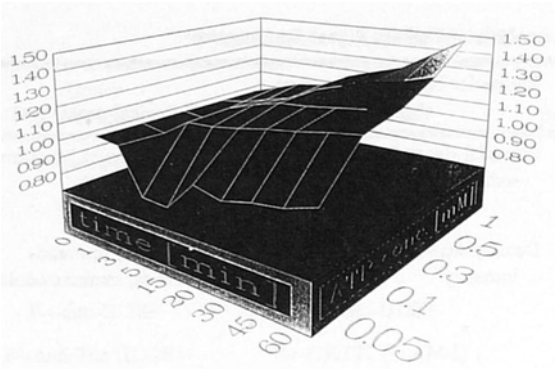

Fig. 5. Flow cytometric analysis of the biphasic character of extracellular ATP-induced membrane potential changes in murine thymocytes. A three-dimensional plot of the normalized membrane potential of cells, determined from oxonol-fluorescence histograms, as a function of the ATP concentration and incubation time. The 1.0 value on the *Z* axis represents the resting membrane potential of the cells.

onol-fluorescence histograms recorded by flow cytometry [59].

Intracellular Ion Concentrations

Flow cytometry is also often used to determine changes in intracellular ion concentrations, such as Ca^{2+} or H^+. The procedure is based on loading of acetoxymethylester derivatives of fluorescent indicators into the cells and subsequent recording of fluorescence intensities upon dual-color excitation (or at two emission wavelengths upon single-wavelength excitation) in the ratiometric mode. Flow cytometry also allows kinetic measurements of transient rises of $[Ca^{2+}]_i$ in the real-time data acquisition mode. The use of different probes and the technical details have recently been extensively reviewed [52,53,55,58]. The latest developments introduced several nonratiometric fluorochromes (e.g., FLUO-3) and their ratio-mode versions (FLUORHOD) [60] to Ca^{2+} measurements in the visible wavelength range; these avoid problems associated with the use of UV probes [61,62]. With the unique property of fast heterogeneity analysis for a large cell population, flow cytometry provides a powerful tool for studying Ca^{2+} signaling.

Multiparameter Kinetic Analysis of Complex Signal Transmission Processes

Flow cytometry also offers the possibility of kinetic analysis of complex signaling processes such as programmed cell death (apoptosis) by means of correlated multiparameter data acquisition and evaluation. This process is accompanied by changes in membrane permeability, membrane potential, intracellular calcium level, cell volume, granularity and by fragmentation of nuclear DNA. These events are usually ordered in a sequence and occur several minutes or hours after the triggering signal. Flow cytometric analysis of the process requires multiple staining of the cells. Membrane permeability changes can be nicely detected by measuring the kinetics of intracellular accumulation of DNA dyes (Hoechst 33342, ethidium bromide, propidium iodide) [63–65] or by a simultaneous application of two vital dyes, fluorescein diacetate (FDA) and propidium iodide [66]. The combination of permeability probes with potential-sensitive dyes and simultaneous measurement of forward and/or side-scatter signals allows a complex, multiparameter kinetic analysis of apoptosis [64,67] and a discrimination of necrosis and apoptosis [64]. Figure 6 illustrates the flow cytometric kinetic analysis of the initial phases of extracellular ATP-triggered apoptosis [59] in murine medullary thymocytes, using the fluorescence signal of oxonol dye to detect depolarization and the forward-angle light scatter signal to detect a decreased cell volume.

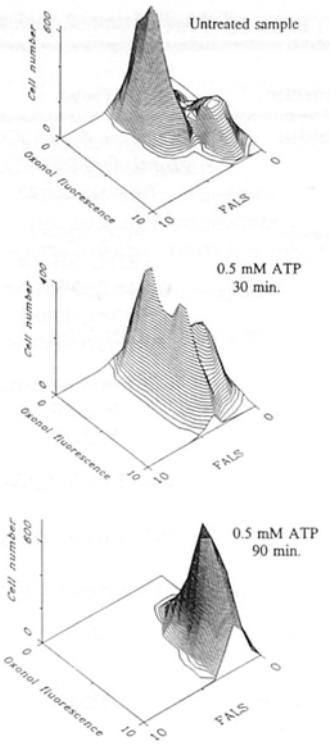

Fig. 6. Flow cytometric analysis of the early phases of extracellular ATP-triggered apoptosis in murine thymocytes. The three-dimensional plot shows an increasing fraction of cells with higher oxonol fluorescence (depolarized state) and lower forward-angle light scatter (smaller volume) at the increasing incubation times.

FUTURE TRENDS IN FLOW CYTOMETRY

The currently used flow cytometers are still susceptible to major improvements. The computer hardware and detectors are no longer the limiting factor. The design of better fluorescent probes and more versatile ligands is expected, allowing simultaneous detection of even more parameters. One very promising direction is the construction of flow cytometers capable of measuring fluorescence lifetimes using the phase shift method [68]. This technique might be very useful in suppressing the interferences caused by autofluorescence, nonspecific dye binding, unbound fluorescent dyes, and even light scattering [69].

ACKNOWLEDGMENTS

The authors gratefully acknowledge the excellent technical assistance of Ms. Á. Gara, A. Harangi, and T. Wei. The helpful and stimulating discussions with Drs. M. Edidin, T. M. Jovin, D. J. Arndt-Jovin, M. Balázs, G. Vereb, and G. Panyi are also greatly appreciated. This work was supported by OTKA grants (1492, 6221, and 6163), ETT 469, and the U.S.–Hungarian Joint Fund for Science and Technology (JF-294 and JF-292).

REFERENCES

1. M. R. Melamed, P. F. Mullaney, and M. L. Mendelsohn (Eds.) (1979) *Flow Cytometry and Sorting*, John Wiley & Sons, New York.
2. H. M. Shapiro (1985) *Practical Flow Cytometry*, Alan R. Liss, New York.
3. M. A. Van Dilla, P. N. Dean, O. D. Laerum, and M. R. Melamed (Eds.) (1985) *Flow Cytometry: Instrumentation and Data Analysis*, Academic Press, London.
4. L. A. Herzenberg, R. G. Sweet, and L. A. Herzenberg (1976) *Sci. Am.* **234**(3), 108.
5. D. J. Arndt-Jovin and T. M. Jovin (1978) *Annu. Rev. Biophys. Bioeng.* **7**, 527.
6. M. J. Fulwyler (1980) *Blood Cells* **6**, 173.
7. O. D. Laerum and T. Farsund (1981) *Cytometry* **2**, 1.
8. J. A. Steinkamp (1984) *Rev. Sci. Instrum.* **55**, 1375.
9. K. A. Ault (1983) *Diagnost. Immunol.* **1**, 2.
10. E. J. Lovett, III, B. Schnitzer, D. F. Keren, A. Flint, J. L. Hudson, and K. D. McClatchey (1984) *Lab. Invest.* **50**, 115.
11. F. Traganos (1984) *Cancer Invest.* **2**(2), 149.
12. F. Traganos (1984) *Cancer Invest.* **2**(3), 239.
13. K. A. Muirhead, P. K. Horan, and G. Poste (1985) *Bio/Technology* **3**, 337.
14. D. R. Parks, L. L. Lanier, and L. A. Herzenberg (1986) in D. M. Weir, C. C. Blackwell, L. A. Herzenberg, and L. A. Herzenberg (Eds.), *Handbook of Experimental Immunology*, Blackwell Scientific, Edinburgh. Vol. 1, pp. 29.1.
15. L. Mátyus and M. Edidin (1991) in J. R. Lakowicz (Ed.), *Topics in Fluorescence Spectroscopy*, Plenum Press, New York, p. 441.
16. A. N. Glazer and L. Stryer (1983) *Biophys. J.* **43**, 383.
17. B. Prezelin and F. I. Haxo (1976) *Planta (Berl.)* **128**, 133.
18. J. E. Aubin (1979) *J. Histochem. Cytochem.* **27**, 36.
19. R. C. Benson, R. A. Meyer, M. E. Zaruba, and G. M. McKhann (1979) *J. Histochem. Cytochem.* **27**, 44.
20. J. A. Steinkamp and C. C. Stewart (1986) *Cytometry* **7**, 566.
21. M. Roederer and R. F. Murphy (1986) *Cytometry* **7**, 558.
22. S. Alberti, D. R. Parks, and L. A. Herzenberg (1987) *Cytometry* **8**, 114.
23. J. P. Corsetti, S. V. Sotirchos, C. Cox, J. W. Cowles, J. F. Leary, and N. Blumburg (1988) *Cytometry* **9**, 539.
24. T. Förster (1949) *Z. Naturforsch. A. Astrophys. Phys. Phys. Chem.* **4**, 321.
25. R. A. Marcus and N. Sutin (1985) *Biochim. Biophys. Acta* **811**, 265.
26. L. Mátyus (1992) *J. Photochem. Photobiol. B Biol.* **12**, 323.
27. J. Matkó, A. Jenei, L. Mátyus, M. Ameloot, and S. Damjanovich (1993) *J. Photochem. Photobiol. B Biol.* **19**, 69.
28. L. Stryer (1978) *Annu. Rev. Biochem.* **47**, 819.
29. S. Damjanovich, J. Szöllősi, and L. Trón (1992) *Immunol. Today* **13**, A12.
30. G. Vereb, R. E. Dale, L. Mátyus, L. Bene, G. Panyi, Zs. Bacsó, M. Balázs, J. Matkó, C. Pieri, M. Ameloot, J. Szöllősi, R. Gáspár, and S. Damjanovich (1994) *J. Mol. Recogn.* (in press).
31. L. Trón, J. Szöllősi, S. Damjanovich, H. Helliwell, D. J. Arndt-Jovin, and T. M. Jovin (1984) *Biophys. J.* **45**, 929.
32. R. Zidovetzki, Y. Yarden, J. Schlessinger, and T. M. Jovin (1981) *Proc. Natl. Acad. Sci. USA* **78**, 6981.
33. R. E. Dale, J. Eisinger, and W. E. Blumberg (1979) *Biophys. J.* **26**, 161.
34. R. A. Marcus (1956) *J. Chem. Phys.* **24**, 966.
35. D. L. Dexter (1953) *J. Chem. Phys.* **21**, 836.
36. J. J. Hopfield (1974) *Proc. Natl. Acad. Sci. USA* **71**, 3640.
37. P. Maróti (1993) *J. Photochem. Photobiol. B. Biol.* **19**, 235.
38. J. N. Betts, D. N. Beratan, and J. N. Onuchic (1992) *J. Am. Chem. Soc.* **114**, 4043.
39. J. Matkó, K. Ohki, and M. Edidin (1991) *Biophys. J.* **59**, 126a.
40. J. Matkó, K. Ohki, and M. Edidin (1992) *Biochemistry* **31**, 703.
41. S. A. Green, D. J. Simpson, G. Zhou, P. S. Ho, and N. V. Blough (1990) *J. Am. Chem. Soc.* **112**, 7337.
42. J. Matkó, A. Jenei, T. Wei, and M. Edidin (1994) *Cytometry* (in press).
43. J. Matkó, Y. Bushkin, T. Wei, and M. Edidin (1994) *J. Immunol.* **152**, 3353.
44. A. Chakrabarti, J. Matkó, N. A. Rahman, B. G. Barisas, and M. Edidin (1992) *Biochemistry* **31**, 7182.
45. K. Wyatt and R. J. Cherry (1992) *Biochemistry* **31**, 4650.
46. S. Papp, S. Pikula, and A. Martonosi (1987) *Biophys. J.* **51**, 205.
47. M. Edidin and T. Wei (1982) *J. Cell Biol.* **95**, 458.
48. S. S. Chan, D. J. Arndt-Jovin, and T. M. Jovin (1979) *J. Histochem. Cytochem.* **27**, 56.
49. J. Szöllősi, L. Trón, S. Damjanovich, H. Helliwell, D. J. Arndt-Jovin, and T. M. Jovin (1984) *Cytometry* **5**, 210.
50. J. Matkó, J. Szöllősi, L. Trón, and S. Damjanovich (1988) *Q. Rev. Biophys.* **21**, 479.
51. B. Alberts, D. Bray, J. Lewis, M. Raff, K. Roberts, and J. D. Watson (1989) *Molecular Biology of the Cell*, Garland, New York & London, Chap. 12.
52. H. M. Shapiro (1988) *Practical Flow Cytometry*, 2nd ed., Alan R. Liss Inc., New York.
53. M. R. Melamed, T. Lindmo, and M. L. Mendelsohn (Eds.) (1990) *Flow Cytometry and Sorting*, Wiley & Liss, New York.
54. A. Waggoner (1986) in D. Lansing Taylor, A. S. Waggoner, F. Lanni, R. F. Murphy, and R. R. Birge (Eds.), *Application of Fluorescence in Biomedical Sciences*, Alan R. Liss, New York, p. 3.
55. R. Y. Tsien (1989) *Methods Cell Biol.* **30**, 127.
56. R. P. Haugland (1992–1994) *Handbook of Molecular Probes*, Molecular Probes, Eugene, OR.
57. M. Edidin (1989) *Methods Cell Biol.* **29**, 87.
58. T. M. Chused, H. A. Wilson, B. E. Seligmann, and R. Y. Tsien (1986) in D. Lansing Taylor, A. S. Waggoner, F. Lanni, R. F.

Murphy, and R. R. Birge (Eds.), *Application of Fluorescence in Biomedical Sciences*, Alan R. Liss, New York, p. 531.
59. J. Matkó, P. Nagy, Gy. Panyi, Gy. Vereb Jr., L. Bene, L. Mátyus, and S. Damjanovich (1993) *Biochem. Biophys. Res. Commun.* **191**, 378.
60. G. A. Smith, J. C. Metcalfe, and S. D. Clarke (1993) *J. Chem. Soc. Perkin Trans.* **2**, 1195.
61. G. T. Rijkers, L. B. Justement, A. W. Griffioen, and J. C. Cambier (1990) *Cytometry* **11**, 923.
62. P. A. Vandenberghe and J. L. Ceuppens (1990) *J. Immunol. Methods* **127**, 197.
63. M. G. Ormerod, X.-M. Sun, R. G. Snovden, R. Davies, H. Fearnhead, and G. M. Cohen (1993) *Cytometry* **14**, 595.
64. C. Dive, C. D. Gregory, D. J. Phipps, D. L. Evans, A. E. Milner, and A. H. Wyllie (1992) *Biochim. Biophys. Acta* **1133**, 275.
65. V. N. Afanasyev, B. A. Korol, N. P. Matylevich, V. A. Pechatnikov, and S. R. Umanski (1993) *Cytometry* **14**, 603.
66. L. Mátyus, G. Szabó Jr., I. Resli, R. Gáspár Jr., and S. Damjanovich (1984) *Acta Biochim. Biophys. Acad. Sci. Hung.* **19**, 209.
67. Z. Darzynkiewicz, S. Bruno, G. Del Bino, W. Gorczyca, M. A. Hotz, P. Lassota, and F. Traganos (1992) *Cytometry* **13**, 795.
68. B. G. Pinsky, J. J. Ladasky, J. R. Lakowicz, K. Berndt, and R. A. Hoffman (1993) *Cytometry* **13**, 123.
69. J. A. Steinkamp and H. A. Crissman (1993) *Cytometry* **14**, 210.
70. D. M. Jenis, A. L., Stepanowski, O. C. Blair, D. E. Burger, and A. C. Sartorelli (1984) *J. Cell Physiol.* **121**, 501.
71. J. Szöllósi, L. Mátyus, L. Trón, M. Balázs, I. Ember, M. J. Fulwyler, and S. Damjanovich (1987) *Cytometry* **8**, 120.
72. S. Damjanovich, L. Trón, J. Szöllósi, R. Zidovetzki, W. L. C. Vaz, F. Regateiro, D. J. Arndt-Jovin, and T. M. Jovin (1983) *Proc. Natl. Acad. Sci. USA* **80**, 5985.
73. J. Szöllósi, S. Damjanovich, C. K. Goldman, M. J. Fulwyler, A. Aszalós, G. Goldstein, and T. A. Waldmann (1987) *Proc. Natl. Acad. Sci. USA* **84**, 7246.
74. J. Szöllósi, F. M. Brodsky, M. Balázs, P. Nagy, L. Trón, M. J. Fulwyler, and S. Damjanovich (1989) *J. Immunol.* **143**, 208.
75. A. P. Harel-Bellan, P. Krief, L. Rimsky, W. L. Farrar, and Z. Mishal (1990) *Biochem. J.* **268**, 35.
76. T. Liegler, J. Szöllósi, W. Hyun, and R. S. Goodenow (1991) *Proc. Natl. Acad. Sci USA* **88**, 6755.
77. R. S. Mittler, S. J. Goldman, G. L. Spitalny, and S. J. Burakoff (1989) *Proc. Natl. Acad. Sci. USA* **86**, 8531.
78. R. S. Mittler, B. M. Rankin, and P. A. Kiener (1991) *J. Immunol.* **147**, 3434.
79. J.-P. Gorvel, Z. Mishal, F. Liegey, A. Rigal, and S. Maroux (1989) *J. Cell Biol.* **108**, 2193.